A Study on the Bond Characteristics of Steel Bars in Concrete Containing Polypropylene (PP) Plastic Particles as Fine Aggregate

Muhammad Sofyan
Civil Engineering Department, Universitas Hasanuddin, Makassar, Indonesia
m.sofyan@itpln.ac.id

Herman Parung
Civil Engineering Department, Universitas Hasanuddin, Makassar, Indonesia
parungherman@yahoo.com

Muhammad Wihardi Tjaronge
Civil Engineering Department, Universitas Hasanuddin, Makassar, Indonesia
tjaronge@yahoo.co.jp

Andi Arwin Amiruddin
Civil Engineering Department, Universitas Hasanuddin, Makassar, Indonesia
arwin_amiruddin@unhas.ac.id (corresponding author)

Received: 28 July 2024 | Revised: 12 August 2024 | Accepted: 14 August 2024

 DOI: https://doi.org/10.48084/etasr.8544

ABSTRACT

The use of plastic in modern society has resulted in a considerable amount of environmental contamination, largely due to the inherent chemical composition of the material. This poses a significant risk to the surrounding environment, particularly in terms of its impact on soil, air, and water quality. The use of recycled plastic in concrete is becoming increasingly prevalent within the construction industry due to its potential to mitigate environmental contamination from plastic waste. The objective of this study was to evaluate the performance of concrete incorporating recycled Polypropylene (PP) plastic as a fine aggregate. The two critical factors under examination were the quantity of PP plastic granules used as a proportion of fine aggregate (ranging from 0% to 30%) and the water-cement (w/c) ratio, which could be 0.45 or 0.55, in conjunction with a 1.5% plasticizer. The samples were subjected to a pull-out test to evaluate the parameters of bond stress behavior, failure mode, and bond-slip behavior. The findings indicated that an increase in the proportion of PP plastic granules used as a substitute for fine aggregate resulted in a notable reduction in bond strength, which was further amplified when the w/c ratio was diminished. The incorporation of 10% PP plastic granules led to a reduction in bond stress by 13.4% and 11.56%, respectively, in samples with w/c ratios of 0.45 and 0.55. Consequently, at a low w/c ratio, the predominant failure mode is considered to be splitting, while a higher w/c ratio increases the probability of pull-out splitting failure.

Keywords-concrete; bond strength; polypropylene; bond-slip behavior; failure mode

I. INTRODUCTION

The global utilization of plastic is undergoing an exponential growth, resulting in a notable surge in plastic waste and giving way to mounting ecological concerns [1, 2]. In general, the plastic contamination of the land, air, and water is caused by the toxic chemical composition of the material, which poses significant environmental risks [3, 4]. Furthermore, this waste material obstructs streams and contributes to flooding, thereby creating an environment conducive to the propagation of mosquito-borne diseases. Among the various countries, Indonesia is projected to be the second largest source of plastic pollution in the maritime environment, after China [5, 6]. It is estimated that approximately 3.22 million metric tons (MMT) of plastic are contributed to the marine environment by Indonesia on an annual basis [6]. The management of plastic waste can be achieved through three principal methods: recycling, incineration (typically with energy recovery), and disposal [7]. In 2015, 27.3% of plastic waste in Europe was deposited in

landfills [8], while in the United States, this figure reached 75.4% of 35.4 million tons. Given the abundance of these materials, several investigations have been conducted to assess the performance of three types of plastic in concrete: polypropylene (PP), polyethylene terephthalate (PET) [9, 10], and high-density polyethylene (HDPE) [11]. These diverse plastic elements may be repurposed into construction materials in different forms, including fibers and aggregates. The incorporation of PP fibers into concrete has proven to enhance the mechanical qualities and durability of the resulting material [12, 13]. The findings indicated that the incorporation of Recycled Plastic Fiber (RPF) markedly augmented the capacity to withstand loads and mitigated the shrinkage associated with drying, particularly during the initial phases. This demonstrated that RPF could be employed in the fabrication of robust, long-lasting, and environmentally friendly building materials [14-16]. Furthermore, when up to 30% of traditional aggregates are substituted with PP plastic, concrete exhibits sufficient mechanical qualities, despite a slight reduction in compressive strength. Nevertheless, the incorporation of PP can facilitate a reduction in the overall weight of concrete [17]. The use of recycled plastic milk bottle fibers and an altered surface texture has been demonstrated to enhance the resilience of the composite material [18]. The use of recycled plastic as a fine aggregate in sustainable three-dimensional concrete printing displayed certain attributes [19]. However, the incorporation of recycled plastic as an aggregate in concrete exhibited a more substantial usage amount in comparison to RPF. Furthermore, the utilization of waste as an aggregate has the potential to significantly reduce the volume of waste generated, making it a viable and practical solution. Consequently, the process of converting recycled plastic into aggregate is inherently labor-intensive, necessitating a significant input to achieve the desired qualities [20-23].

The performance of Reinforced Concrete (RC) buildings is typically contingent upon the interaction between the concrete and the steel reinforcement. In order to achieve the desired concrete strength, it is essential for the reinforcing material to exhibit robust tensile and bond strength. The use of high-strength RC can effectively reduce the cross-sectional dimensions of components, thereby enhancing structural integrity and optimizing concrete capacity. It is therefore substantial to ensure that the reinforcing steel and concrete components are properly bonded in order to guarantee their effective contribution to structural stability [24]. An indispensable criterion for attaining the optimal design of RC structures is the efficient and reliable transmission of loads from the reinforcement to the adjacent concrete [25]. In addition, the bond performance between concrete and reinforcement can be adversely affected by three significant factors. These include, the phenomenon of reinforcement slip, which arises from the deterioration of the chemical adhesion between the concrete and the reinforcement surface. Secondly, pull-out of reinforcement is caused by the deterioration of concrete in the vicinity of and between the reinforcement locks. Thirdly, the slanted orientation of the ribs results in a force acting on the reinforcement, generating a radial stress perpendicular to the axis of the reinforcement. This leads to the failure of concrete in split-tensile. A number of studies have been conducted with the objective of evaluating the bonding characteristics of steel reinforcement embedded in concrete. The influence of distinct mixtures, including plastic waste and steel fibers, on these variables has also been evaluated individually. A prior study conducted a pull-out test to examine the relationship between steel reinforcement and concrete incorporating rubber waste at approximately 30% of the aggregate weight [26]. The results were presented in the form of a load-slip relationship graph and a bond strength-rubber waste content graph, which revealed a significant decrease in bond strength with increasing the waste content.

An investigation was conducted to examine the bond characteristics of steel reinforcement embedded in concrete, with a particular focus on the impact of other substances, including plastic waste and steel fibers. The objective of the experiments was to investigate the correlation between steel reinforcement and concrete, including rubber waste comprising 30% of the aggregate weight. The results were presented in the form of a load-slip relationship graph and a bond strength-rubber waste content graph, which revealed a significant correlation between an increase in the waste content and a decrease in bond strength [26]. Other empirical evidence [27-29], indicate that steel fibers enhance the rigidity and adhesive properties of concrete, thereby improving its hardness and bond performance. Specifically, as the Vertical stress field (Vsf) increased, the applied load required to cause failure in Steel Fiber-Reinforced Concrete (SFRC) specimens exhibited a 7-16% improvement. Another study also investigated the bond-slip characteristics of epoxy-coated reinforcement in Ultra-High-Performance Concrete (UHPC) with steel fibers [30]. The findings indicated that the bond-slip behavior of epoxy-coated reinforcement in UHPC was comparable to that of reinforcement in Normal-Strength Concrete (NSC). A comprehensive mathematical model was presented for the bond-slip curve in both tension and compression.

Authors in [31] investigated the influence of Recycled Concrete Aggregate (RCA) on concrete bonding strength and observed that concrete incorporating RCA exhibited diminished bonding strength in comparison to conventional concrete. Authors in [32] obtained analogous results, wherein the incorporation of RCA and pozzolanic materials influenced the compressive strength, durability, and bonding strength of reinforcement in concrete. The research reveals a number of shortcomings, including the lack of comparative studies on diverse plastic varieties, such as PP granules in concrete, the limited examination of PP granules as a fine aggregate, and the scarcity of data on the impact of PP on bond-slip behavior and structural integrity in reinforced concrete. This study examines the utilization of PP plastic granules as a replacement for fine aggregate in concrete, with a particular focus on assessing their influence on the bond strength between concrete and reinforcing steel. This approach is innovative in comparison to previous research, which has primarily focused on distinct categories of plastic waste, such as PET and HDPE, or alternative forms of recycled materials, such as rubber waste and RCA, rather than PP granules. This paper presents novel empirical equations and bond-slip behavior models specifically for concrete that incorporates PP granules, a topic that has not been fully investigated in previous literature. This provides a

novel perspective on the impact of diverse forms of plastic waste on the structural characteristics of concrete.

II. MATERIALS AND METHOD

A. Materials

The primary binder used in this investigation was Portland composite cement, manufactured by PT Semen Tonasa Indonesia, with a specific gravity of 3.01. The coarse aggregate used in this study was obtained from crushed stone with a maximum size of 19 mm. Meanwhile, the fine aggregate was procured from nearby material retailers for use in the mixture and examined in accordance with the ASTM C136-01 criteria, as presented in Table I. The admixture employed is SikaCim Concrete Additive, a plasticizer manufactured by Sika. It is classified as a high-range water-reducing additive, designed exclusively for use in the concrete industry. Its primary chemical component is modified naphthalene formaldehyde sulfonate. The admixture facilitates the expeditious removal of formwork while simultaneously obtaining a higher initial compressive strength, demonstrating optimal efficacy across all recommended dosage levels. The primary objective of incorporating the superplasticizer was to achieve the desired level of fluidity, as specified by a slump range of 80-120 mm, while simultaneously maintaining a low water-to-cement ratio. The plasticizer is a liquid with a density of 1.17 ± 0.01 kg/L (at +20°C) and a dark brown coloration. The plastic material used is PP, which has undergone a transformation into granules exhibiting a uniform particle size of 3 mm and a dry density of 515.25 kg/m³, as shown in Figure 1. The recycling of PP plastic into granules or pellets commences with the collection and classification of discarded plastic, followed by a cleaning process to remove impurities. The original plastic is then fragmented into minuscule particles, liquefied, and forced through a narrow opening to create filaments. The filaments are fragmented into small granules or pellets, which are subsequently subjected to a chilling, dehydration, and packaging process for recycling as primary ingredients in a variety of plastic products.

TABLE I. PROPERTIES OF FINE AND COARSE AGGREGATE

Properties	Units	Aggregate	
		Fine Aggregate	Coarse Aggregate
Fine Modulus	%	2.44	5.96
Apparent Specific Gravity	-	2.42	2.71
Bulk Specific Gravity	-	2.25	2.54
SSD Specific Gravity	-	2.32	2.6
Water Absorption	%	3.1	2.48
Water Content	%	3.4	1.78
Clay Content	%	1.58	5.36
Aggregate Abrasion	%	-	26.75
Dry Density	kg/ltr	1.34	1.27

The RILEM RC6 [33] guidelines were followed in the conduct of pull-out testing. In the initial stage of the experiment, the bond length (l_d) was set to a value that was five times the diameter of the reinforcement ($5d_s$), while the diameter of the reinforcement (d_s) was assigned a constant value of 16 mm.

Fig. 1. Polypropylene (PP) granules.

B. Method

The concrete sample is a cubic form with dimensions of (160×160×160) mm, in accordance with the RILEM RC6 recommendation of measuring the length, breadth, and height of the cube at 10 d_s. The reinforcement employed is a threaded reinforcement, as evidenced in Figure 2, which depicts the configuration of the sample and the apparatus used for the pull-out test. The RILEM RC6 method is employed to conduct a pull-out test, the objective of which is to quantify the bond strength between concrete and steel reinforcement. A steel reinforcement bar is embedded in a concrete beam at a prescribed length. The sample is positioned within a testing apparatus, wherein a constant axial tensile force is applied to the unrestrained end of the reinforcement until either slippage or bond failure occurs. The degree of slippage is quantified, and the maximum load at which failure occurs is recorded during the test. The data are employed to ascertain the binding strength and to analyze the slip behavior between concrete and reinforcement. The mix design in this study was established in accordance with the specifications set forth in the Indonesian standard [34]. A total of eight samples were created in this study, with a water-to-cement ratio of 0.45 and 0.55, respectively. The proportion of PP plastic granules used as a substitute of sand varies at distinct levels: 0%, 10%, 20%, and 30% of the fine aggregate volume. The plasticizer is incorporated into the mixture at a concentration of 1.5% relative to the weight of the cement, as presented in Table II, which depicts the sample mix design. The concrete mix design

was formulated in accordance with the specifications outlined in the SNI 03-2834-2000 standard or procedure [35].

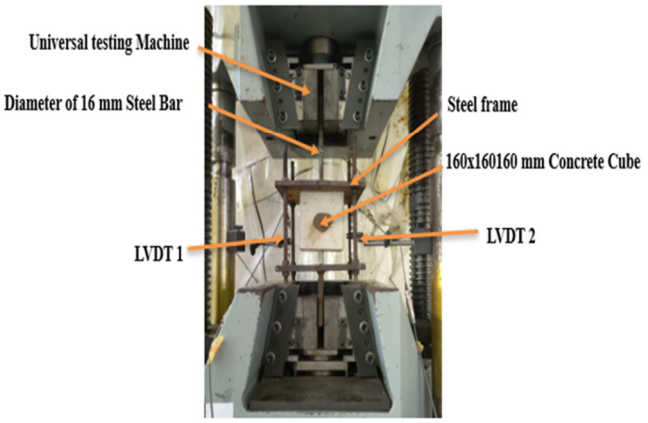

Fig. 2. Pull out test configuration.

TABLE II. MIX DESIGN

Mix ID	Cement (kg/m^3)	Fine Aggregate (kg/m^3)	Coarse Aggregate (kg/m^3)	Water (kg/m^3)	PP Granules Content (kg/m^3)
PL0-0.45	455.56	854.96	874.86	205	0
PL0-0.55	372.73	909.67	894.32	205	0
PL10-0.45	455.56	769.46	874.86	205	17.75
PL10-0.55	372.73	818.7	894.32	205	18.89
PL20-0.45	455.56	683.96	874.86	205	35.51
PL20-0.55	372.73	727.73	894.32	205	37.78
PL30-0.45	455.56	598.47	874.86	205	53.26
PL30-0.55	372.73	636.77	894.32	205	56.67

RILEM RC6 [33] introduces an equation to determine the average bond stress along the embedment length of the bar (l_b), based on the tensile force (F) in the pull-out test (1) and d_s is the diameter of the rebar (mm). This equation calculates the average bond stress across the embedment length of the bar due to the non-uniform distribution of the parameter:

$$\tau = \frac{F}{5.\pi.d_s^2} \quad (1)$$

The CEB-FIP Model Code recommends a model that is highly universal for defining bond-slip behavior, as depicted in Figure 3. This model delineates the comprehensive bond-slip characteristics across multiple stages, thereby facilitating a comprehensive understanding of the reinforced bond performance in concrete. Equation (2) may be employed to calculate the bond stress in accordance with this model [36], wherein f'_c represents the compressive strength of concrete:

$$\tau = 2.5\sqrt{f'c} \quad (2)$$

III. RESULTS AND DISCUSSION

A. Bond Strength and Bond-Slip Behavior

An investigation was conducted to examine the impact of PP granule content on bond stress by varying the water-to-cement (w/c) ratio and the proportion of plastic granules. As shown in Figure 4, an increase in PP plastic granules by 10% resulted in a reduction in bond stress on the surface of the reinforcing steel rods. The control sample, which contained no PP plastic granules, demonstrated the greatest binding effectiveness across all w/c ratios. Moreover, as the water-to-cement ratio decreased, the bond stress value demonstrated an upward trajectory.

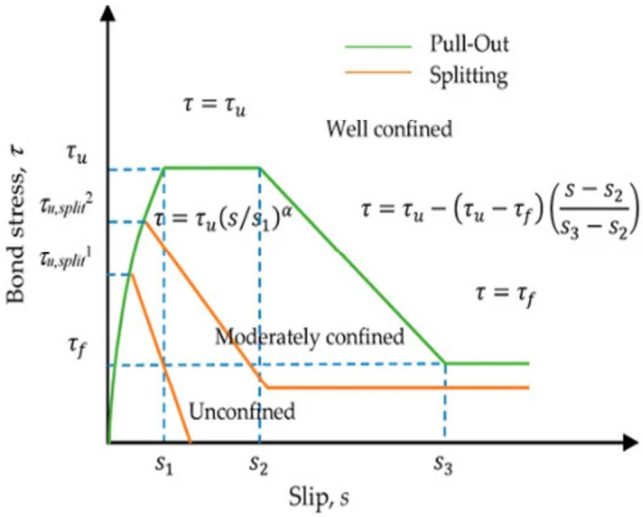

Fig. 3. Analytical bond-slip behavior [36].

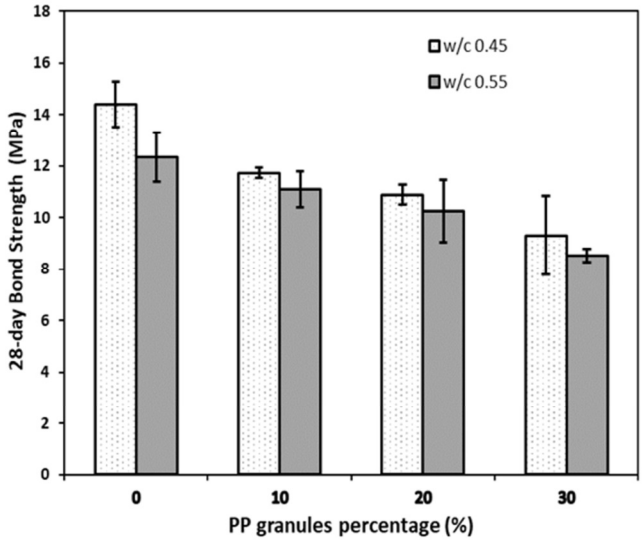

Fig. 4. 28-day bond strength of sample.

As the water-to-cement ratio (w/c ratio) increases, a greater quantity of water is added in relation to the amount of cement. Following the mixing process, a higher w/c ratio results in a greater volume of water evaporating, leaving behind a greater number of voids or pores within the hardened concrete. This increased porosity results in a reduction in the density of the concrete, which consequently weakens the material's overall structural integrity, including the bond strength. The interface between PP and the cement paste may not be as strong as the interface between traditional aggregates and the cement paste.

The implementation of PP can introduce additional voids or weak points in the matrix, which in turn leads to a reduction in bond strength. The analysis of the deformation observed in the sample was conducted by establishing a correlation between the bond stress and the slip. As illustrated in Figure 5, a bond stress-against-slip relationship was observed at a w/c ratio of 0.45. The majority of curves exhibit a pronounced incline during the initial loading phase, reaching the ultimate stress level. This indicates that the combined effects of chemical adhesion and static friction facilitate the transmission of applied stress from the reinforcement to the concrete. The slip behavior exhibited a consistent pattern. This indicates that the slip process is predominantly influenced by the interaction between the concrete and reinforcement, rather than solely by bond tension. The PL30-0.45 sample, comprising 30% PP granules, exhibited the highest slip value at the maximum bond stress ($S_{\tau b,max}$), measuring 0.35 mm.

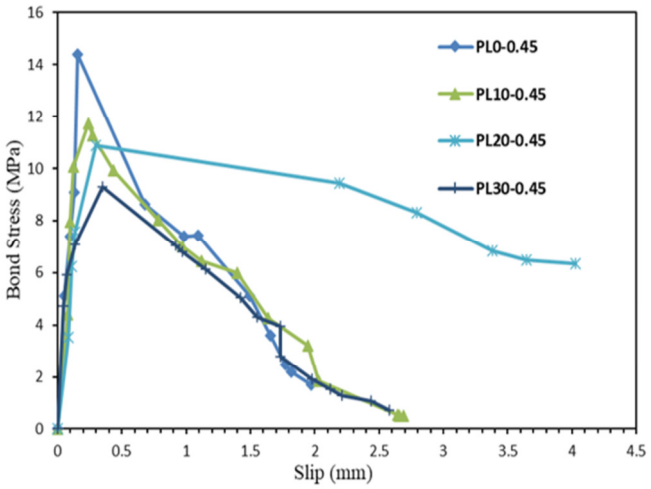

Fig. 5. Bond-slip behavior of w/c ratio 0.45 sample.

A notable increase in the quantity of PP plastic granules in the sample resulted in a higher slip value at the maximum bond stress. The phase subsequent to the peak load exhibited a precipitous curve, indicative of a pronounced reduction in bond stress due to diminished adhesion properties between the reinforcement and concrete. The occurrence of slippage demonstrated a substantial correlation. With the exception of the PL20-0.45 sample, which contains 20% PP plastic granules, the majority of phases subsequent to the peak bond stress exhibit a pronounced curvature. Figure 6 presents a test specimen with a w/c ratio of 0.55, wherein the peak curve exhibits a pronounced incline, remaining below 0.45. Moreover, the curve following the maximum bond stress demonstrates a more gradual slope in comparison to the sample with a w/c ratio of 0.45, which decreases as the slip deformation phase becomes longer and slower. The results demonstrate that when subjected to an identical applied loading pattern, augmented bond stress is associated with diminished slip deformation. In particular, the degree of slip at the peak bond stress is directly influenced by the quantity of PP plastic granules. The results indicate that the sample with the maximum PP plastic granules, namely the PL30-0.55 sample, exhibits the highest $S_{\tau b,max}$ value of 0.374 mm for a w/c ratio of 0.55. This finding is consistent with those of previous investigations [37, 38]. The elevated porosity in the mixture with a water-to-cement ratio of 0.55 gives rise to inferior bonding at the interface, which in turn gives rise to an increase in slip. Conversely, the more compact structure of the mixture with a water-to-cement ratio of 0.45 results in a more robust connection, which in turn leads to decreased sliding.

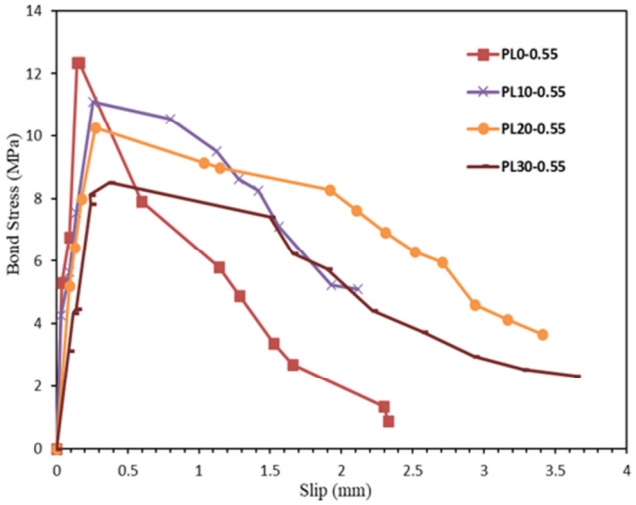

Fig. 6. Bond-slip behavior of w/c ratio 0.55 sample.

The pull-out test demonstrates the failure mechanisms observed in all samples, which can be classified into three distinct types: splitting (S), pull-out/complete pulling out (PO), and a combination of splitting and pull-out (P-S) [39]. Splitting failure, also designated as S failure, manifests as fractures in the surrounding concrete when steel reinforcement is introduced into the concrete matrix. When a tensile force is applied to a material such as concrete, the formation of fractures can occur, with these propagating from the surface of the reinforcement towards the external portion of the concrete. This can result in the concrete breaking or tearing apart around the reinforcement. This phenomenon is typically observed when the bond strength between the reinforcement and the concrete is inadequate to withstand the applied load. It is not uncommon for the pull-out and splitting (P-S) processes to coexist. In a pull-out test, the reinforcement is subjected to forces that seek to extract it from the concrete, resulting in tensile forces. Concurrently, the shear stresses that emerge may lead to the formation of cracks or the detachment of the concrete surrounding the reinforcement, a phenomenon known as splitting. The term "bond slip behavior" is used to describe the interaction between the tensile forces responsible for pull-out and the formation of cracks that result in splitting. These factors collectively impact the bond strength between the concrete and the reinforcement. As portrayed in Figure 7, PO bond failure occurs when stress levels gradually increase, subsequently leading to a decline in the confinement capacity of the concrete in direct contact with the steel reinforcement surface. Given that the tensile forces acting on the reinforcement are relatively low, it is possible to disengage the

reinforcement from the concrete without causing significant cracking. The majority of samples exhibited split failure, as documented in Table III.

Fig. 7. Failure mode of sample.

TABLE III. MECHANICAL PROPERTIES OF PULL-OUT TESTING RESULTS

Sample ID	Bond Strength (MPa)	$S_{\tau b,max}$ (mm)	Failure Mode
PL0-0.45	14.386	0.154	S
PL0-0.55	12.352	0.148	S
PL10-0.45	11.719	0.237	S
PL10-0.55	9.985	0.256	P-S
PL20-0.45	10.885	0.295	P-S
PL20-0.55	10.252	0.271	P-S
PL30-0.45	9.32	0.35	S
PL30-0.55	8.518	0.37	P-S

B. Analytical Model of Bond-Slip Behavior

A number of studies have examined the bond-slip behavior between concrete and reinforcement. The CEB-FIP Model [36, 40, 41] serves as the general models, as shown in Figure 3. This concept is distinguished by four discrete stages. Initially, the bond-slip curve transitions from a state of zero stress to the ultimate bond stress (τ_u) for $s < s_1$. The second stage is characterized by a curve that exceeds the maximum limit while maintaining a steady stress, with a continuous increase in slip. During this period, the stress curve remains constant ($\tau = \tau_u$) for $s_1 < s \leq s_2$, and a significant reduction in stress is observed, followed by an increase in slip when $s_2 < s \leq s_3$. Furthermore, when $s > s_3$, the stress reaches its minimum level and remains constant, indicating complete failure. The experimental results on the samples demonstrated that the phase subsequent to the maximum stress did not exhibit a perfectly flat curve, but rather a diagonal tendency. This finding was supported by the studies conducted by [39-45]. This study proposes the implementation of a modified model based on experimental data, as displayed in Figures 8 and 9. The model commenced at the origin and proceeded to attain the maximum stress, $\tau_{b,max}$, thereby exemplifying a phase characterized by linear stress-slip behavior (Zone 1). Subsequent to the peak stress, the bond stress declines gradually while slip increases, forming a diagonal curve with a moderate slope (Zone 2) when the failure mode is pull-out splitting. The final phase (Zone 3) is distinguished by a notable decline in bond stress, which is then followed by an increase in slip. During this phase, the curve approximates an exponential function.

$$\tau_b = \frac{S.\tau_{b,max}}{S_{\tau b,max}}, 0 < s < s_{\tau b,max} \quad (3)$$

$$\tau_b = \frac{(\tau_{n1}-\tau_{b,max})}{S_{n1}-S_{\tau b,max}}\left(S - S_{\tau b,max}\right) + \tau_{b,max},$$

$$s_{\tau b,max} < s < s_{n1} \quad (4)$$

$$\tau_b = k.a^S, s_{n1} < s < s_{n2} \quad (5)$$

where:

$$k = \frac{\tau_{n2}}{a^{S_{n2}}} \quad (6)$$

$$a^{S_{n2}-S_{n1}} = \frac{\tau_{n2}}{\tau_{n1}} \quad (7)$$

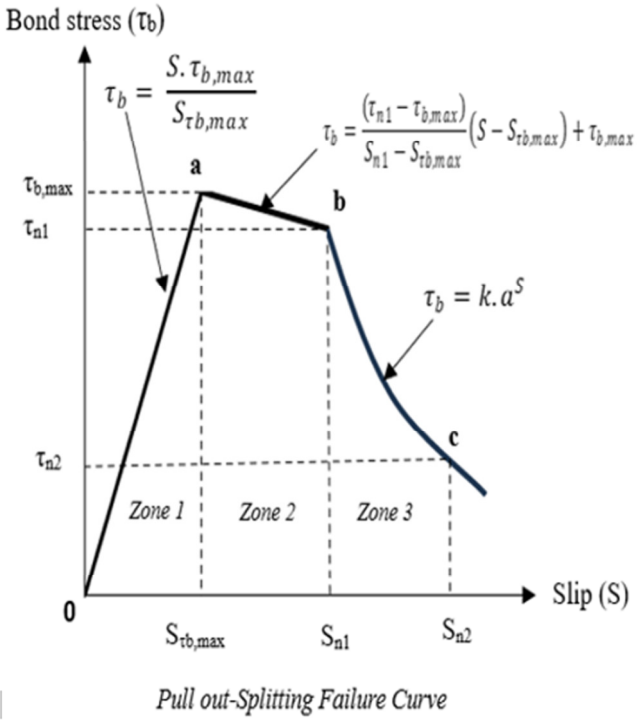

Fig. 8. Proposed model for bond stress-slip relationship (P-S mode).

Figures 10 and 11 show a comparison between the experimental and analytical behaviors associated with the bond slip. The proposed model for each phase is in accordance with the experimental findings for both samples with w/c ratios of 0.45 and 0.55. The majority of curves subsequent to the peak bond stress exhibit a non-flat pattern in contrast to the

preceding model. In particular, the majority of curves in zone 2 are diagonal, as evidenced by the experimental results. In this study, (3), (4), and (5) are employed to generate curves within zones 1, 2, and 3, respectively. The results indicate that the sample that experienced splitting failure did not cross zone 2 due to a significant and sudden reduction in stress.

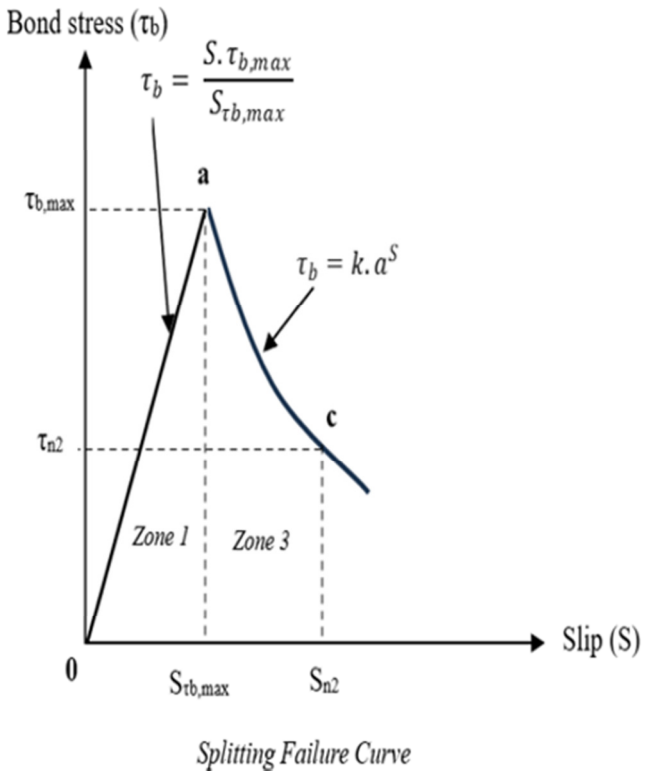

Fig. 9. Proposed model for bond stress-slip relationship (S mode).

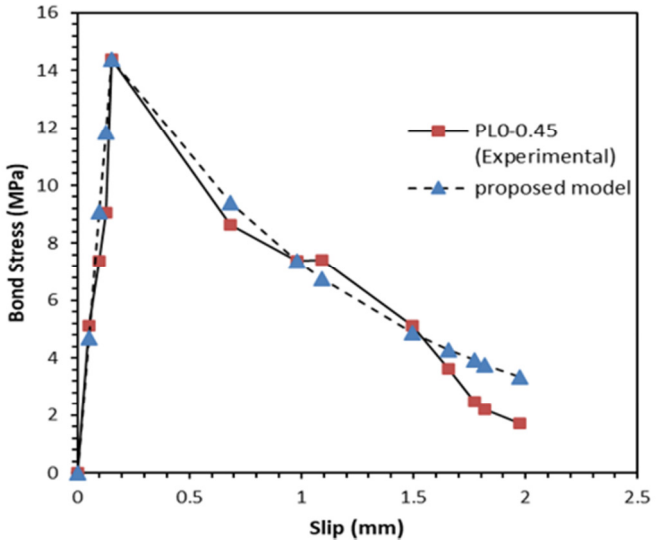

Fig. 10. Comparison between experimental and analytical bond slip behavior for w/c ratio 0.45.

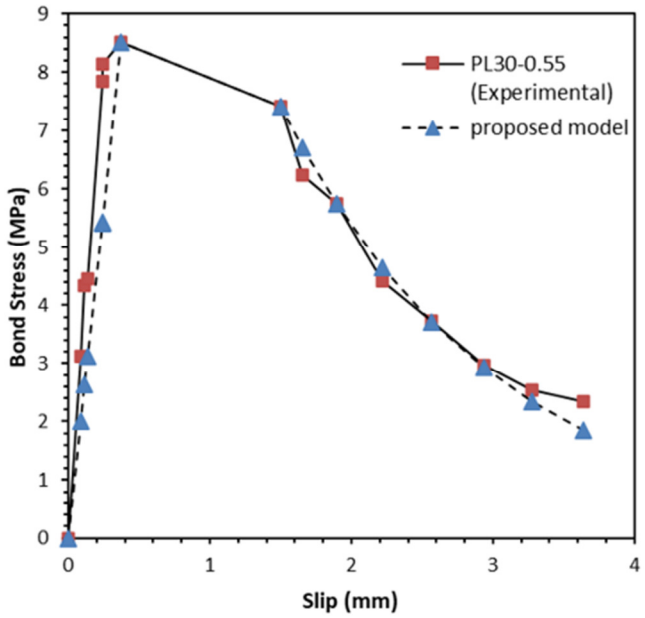

Fig. 11. Comparison between experimental and analytical bond slip behavior for w/c ratio 0.45.

IV. CONCLUSIONS

In conclusion, this study successfully evaluated the performance of concrete including recycled Polypropylene (PP) plastic as a fine aggregate, and the results yielded significant findings as follows:

- The bond stress versus the slip relationship was observed at a w/c ratio of 0.45, demonstrating an inclined, steep trajectory during the initial loading phase. The PL30-0.45 sample, comprising 30% PP plastic granules, exhibited the highest slip value at the maximum bond stress. The results indicated that the bond stress decreased due to a reduction in the adhesion properties between the reinforcement and the concrete, yet slippage still occurred. The PL20-0.45 sample exhibited a relatively mild curvature due to its w/c ratio, with the bond stress declining gradually as the slip deformation phase extended and slowed. Moreover, the quantity of PP plastic granules was found to have a significant impact on the occurrence of slip.
- The pull-out test revealed three distinct failure mechanisms, namely splitting (S), pull-out/complete pulling out (PO), and a combination of splitting and pull-out (P-S), in the samples. A bond failure designated as PO occurred when stress increased, which resulted in a reduction in the concrete's confinement capacity. The majority of samples exhibited a split failure mode, with the PL20-0.45 sample displaying a P-S failure mode due to its ductility. The PL0-0.55 sample exhibited a split failure exclusively due to its 0% PP plastic granule composition, which led to increased brittleness when subjected to loads.
- A comparison of the experimental and analytical bond slip behavior revealed a strong correlation between the predictive model and the experimental data. The model demonstrated non-linear behavior following the attainment

of peak bond stress, exhibiting diagonal curves in zone 2. Furthermore, samples that displayed splitting failure did not traverse zone 2 due to the rapid reduction in stress.

- Novel empirical equations and bond-slip behavior models, specifically tailored for concrete containing PP plastic grains, have been developed. The application of empirical equations and bond-slip models offers a novel perspective on the utilization of PP plastic granules in structural components such as reinforced concrete.

ACKNOWLEDGMENT

This study is supported through funding from YPK PLN/PLN Institute of Technology Jakarta, Indonesia.

REFERENCES

[1] N. Saikia and J. de Brito, "Use of plastic waste as aggregate in cement mortar and concrete preparation: A review," *Construction and Building Materials*, vol. 34, pp. 385–401, Sep. 2012, https://doi.org/10.1016/j.conbuildmat.2012.02.066.

[2] E. Moto *et al.*, "Ecological consequences of microplastic pollution in sub-Saharan Africa aquatic ecosystems: An implication to environmental health," *HydroResearch*, vol. 7, pp. 39–54, Jan. 2024, https://doi.org/10.1016/j.hydres.2023.11.003.

[3] K. U. Donuma, L. Ma, C. Bu, L.-Y. George, M. Gashau, and A. O. Suleiman, "Environmental and human health risks of indiscriminate disposal of plastic waste and sachet water bags in Maiduguri, Borno State Nigeria," *Waste Management Bulletin*, vol. 2, no. 2, pp. 130–139, Jun. 2024, https://doi.org/10.1016/j.wmb.2024.04.002.

[4] M. Qasim, Z. Abbas, and S. K. Abed, "Producing Green Concrete with Plastic Waste and Nano Silica Sand," *Engineering, Technology & Applied Science Research*, vol. 11, no. 6, pp. 7932–7937, Dec. 2021, https://doi.org/10.48084/etasr.4593.

[5] J. H. Tibbetts, "Managing Marine Plastic Pollution: Policy Initiatives to Address Wayward Waste," *Environmental Health Perspectives*, vol. 123, no. 4, pp. A90–A93, 1 April 20, https://doi.org/10.1289/ehp.123-A9.

[6] J. R. Jambeck *et al.*, "Plastic waste inputs from land into the ocean," *Science*, vol. 347, no. 6223, pp. 768–771, Feb. 2015, https://doi.org/10.1126/science.1260352.

[7] J. Gertsakis and H. Lewis, "Sustainability and the Waste Management Hierarchy," 2003.

[8] *An analysis of European plastics production, demand and waste data*. Plastic Europe, 2018.

[9] M. U. Ghani *et al.*, "Mechanical and environmental evaluation of PET plastic-graphene nano platelets concrete mixes for sustainable construction," *Results in Engineering*, vol. 21, Mar. 2024, Art. no. 101825, https://doi.org/10.1016/j.rineng.2024.101825.

[10] A. Shiuly, T. Hazra, D. Sau, and D. Maji, "Performance and optimisation study of waste plastic aggregate based sustainable concrete – A machine learning approach," *Cleaner Waste Systems*, vol. 2, Jul. 2022, Art. no. 100014, https://doi.org/10.1016/j.clwas.2022.100014.

[11] Y. Aocharoen and P. Chotickai, "Compressive mechanical and durability properties of concrete with polyethylene terephthalate and high-density polyethylene aggregates," *Cleaner Engineering and Technology*, vol. 12, Feb. 2023, Art. no. 100600, https://doi.org/10.1016/j.clet.2023.100600.

[12] M. Zhou, X. He, H. Wang, C. Wu, J. He, and B. Wei, "Mechanical properties and microstructure of ITZs in steel and polypropylene hybrid fiber-reinforced concrete," *Construction and Building Materials*, vol. 415, Feb. 2024, Art. no. 135119, https://doi.org/10.1016/j.conbuildmat.2024.135119.

[13] S. Shihada, "Effect of polypropylene fibers on concrete fire resistance," *Journal of Civil Engineering and Management*, vol. 17, no. 2, pp. 259–264, Jun. 2011, https://doi.org/10.3846/13923730.2011.574454.

[14] T.-P. Huynh, T. Ho Minh Le, and N. Vo Chau Ngan, "An experimental evaluation of the performance of concrete reinforced with recycled fibers made from waste plastic bottles," *Results in Engineering*, vol. 18, Jun. 2023, Art. no. 101205, https://doi.org/10.1016/j.rineng.2023.101205.

[15] M. T. Lakhiar, S. Sohu, I. A. Bhatti, N. Bhatti, S. A. Abbasi, and M. Tarique, "Flexural Performance of Concrete Reinforced by Plastic Fibers," *Engineering, Technology & Applied Science Research*, vol. 8, no. 3, pp. 3041–3043, Jun. 2018, https://doi.org/10.48084/etasr.2084.

[16] L. A. Abdulateef, S. H. Hassan, and A. M. Ahmed, "Exploring the Mechanical Behavior of Concrete enhanced with Fibers derived from recycled Plastic Bottles," *Engineering, Technology & Applied Science Research*, vol. 14, no. 2, pp. 13481–13486, Apr. 2024, https://doi.org/10.48084/etasr.6895.

[17] J. Islam and Shahjalal, "Effect of polypropylene plastic on concrete properties as a partial replacement of stone and brick aggregate," *Case Studies in Construction Materials*, vol. 15, Dec. 2021, Art. no. e00627, https://doi.org/10.1016/j.cscm.2021.e00627.

[18] R. Haigh, "The mechanical behaviour of waste plastic milk bottle fibres with surface modification using silica fume to supplement 10% cement in concrete materials," *Construction and Building Materials*, vol. 416, Feb. 2024, Art. no. 135215, https://doi.org/10.1016/j.conbuildmat.2024.135215.

[19] A. J. Babafemi, C. Norval, J. T. Kolawole, S. Chandra Paul, and K. A. Ibrahim, "3D-printed limestone calcined clay cement concrete incorporating recycled plastic waste (RESIN8)," *Results in Engineering*, vol. 22, Jun. 2024, Art. no. 102112, https://doi.org/10.1016/j.rineng.2024.102112.

[20] D. Deti, M. W. Tjaronge, and M. A. Caronge, "Compressive loading and response time behavior of concrete containing refractory brick coarse aggregates," *Journal of Engineering and Applied Science*, vol. 71, no. 1, Apr. 2024, Art. no. 95, https://doi.org/10.1186/s44147-024-00433-7.

[21] U. Jureje, M. W. Tjaronge, and M. A. Caronge, "Basic Engineering Properties of Concrete with Refractory Brick as Coarse Aggregate: Compressive Stress-Time Relationship Assessment," *International Journal of Engineering, Transactions B: Applications*, vol. 37, no. 5, pp. 931–940, May 2024, https://doi.org/10.5829/ije.2024.37.05b.11.

[22] M. Sofyan, A. O. Irlan, A. Rokhman, D. D. Purnama, and R. R. R. Utami, "The Effect of Using Linear Low Density Polyethylene (LLDPE) Powder and Rice Husk Asn on Compressive Strength and Intital Setting Time of Alkaline-Activated Mortar," *IOP Conference Series: Earth and Environmental Science*, vol. 921, no. 1, Nov. 2021, Art. no. 012070, https://doi.org/10.1088/1755-1315/921/1/012070.

[23] L. A. Parsons and S. O. Nwaubani, "Mechanical and durability performance of concrete made using acrylonitrile butadiene styrene plastic from waste-EEE as a partial replacement of the coarse aggregate," *Journal of Building Engineering*, vol. 85, May 2024, Art. no. 108635, https://doi.org/10.1016/j.jobe.2024.108635.

[24] S. Khaksefidi, M. Ghalehnovi, and J. de Brito, "Bond behaviour of high-strength steel rebars in normal (NSC) and ultra-high performance concrete (UHPC)," *Journal of Building Engineering*, vol. 33, Jan. 2021, Art. no. 101592, https://doi.org/10.1016/j.jobe.2020.101592.

[25] *408R-03: Bond and Development of Straight Reinforcing Bars in Tension*. ACI Committee 408, 2003.

[26] M. Gesoglu, E. Güneyisi, O. Hansu, S. İpek, and D. S. Asaad, "Influence of waste rubber utilization on the fracture and steel–concrete bond strength properties of concrete," *Construction and Building Materials*, vol. 101, pp. 1113–1121, Dec. 2015, https://doi.org/10.1016/j.conbuildmat.2015.10.030.

[27] T. A. Söylev, "The effect of fibers on the variation of bond between steel reinforcement and concrete with casting position," *Construction and Building Materials*, vol. 25, no. 4, pp. 1736–1746, Apr. 2011, https://doi.org/10.1016/j.conbuildmat.2010.11.093.

[28] Ş. Yazıcı and S. Arel, "The effect of steel fiber on the bond between concrete and deformed steel bar in SFRCs," *Construction and Building Materials*, vol. 40, pp. 299–305, Mar. 2013, https://doi.org/10.1016/j.conbuildmat.2012.09.098.

[29] L. Huang, Y. Chi, L. Xu, P. Chen, and A. Zhang, "Local bond performance of rebar embedded in steel-polypropylene hybrid fiber reinforced concrete under monotonic and cyclic loading," *Construction and Building Materials*, vol. 103, pp. 77–92, Jan. 2016, https://doi.org/10.1016/j.conbuildmat.2015.11.040.

[30] Z. Zhou and P. Qiao, "Bond behavior of epoxy-coated rebar in ultra-high performance concrete," *Construction and Building Materials*, vol. 182, pp. 406–417, Sep. 2018, https://doi.org/10.1016/j.conbuildmat. 2018.06.113.

[31] L. Butler, J. S. West, and S. L. Tighe, "The effect of recycled concrete aggregate properties on the bond strength between RCA concrete and steel reinforcement," *Cement and Concrete Research*, vol. 41, no. 10, pp. 1037–1049, Oct. 2011, https://doi.org/10.1016/j.cemconres. 2011.06.004.

[32] M. Arezoumandi, T. J. Looney, and J. S. Volz, "Effect of fly ash replacement level on the bond strength of reinforcing steel in concrete beams," *Journal of Cleaner Production*, vol. 87, pp. 745–751, Jan. 2015, https://doi.org/10.1016/j.jclepro.2014.10.078.

[33] "RC6 Bond test for reinforcement steel. 2. Pull-out test," in RILEM Technical Recommendations for the testing and use of construction materials, CRC Press, 1994.

[34] SNI 7656:2012, *Tata cara pemilihan campuran untuk beton normal, beton berat dan beton massa*. BSN, 2012

[35] Tata cara pembuatan rencana beton normal. Standar Nasional Indonesia, 2000.

[36] G. Balázs *et al.*, *Bond and anchorage of embedded reinforcement: Background to the fib Model Code for Concrete Structures 2010*. International Federation for Structural Concrete, 2014.

[37] H. Jeong, S. Ji, J. H. Kim, S.-H. Choi, I. Heo, and K. S. Kim, "Development of Mapping Function to Estimate Bond–Slip and Bond Strength of RC Beams Using Genetic Programming," *International Journal of Concrete Structures and Materials*, vol. 16, no. 1, Sep. 2022, Art. no. 49, https://doi.org/10.1186/s40069-022-00536-6.

[38] D. Gao, H. Yan, D. Fang, and L. Yang, "Bond strength and prediction model for deformed bar embedded in hybrid fiber reinforced recycled aggregate concrete," *Construction and Building Materials*, vol. 265, Dec. 2020, Art. no. 120337, https://doi.org/10.1016/j.conbuildmat. 2020.120337.

[39] M. Fakoor and M. Nematzadeh, "Evaluation of post-fire pull-out behavior of steel rebars in high-strength concrete containing waste PET and steel fibers: Experimental and theoretical study," *Construction and Building Materials*, vol. 299, Sep. 2021, Art. no. 123917, https://doi.org/ 10.1016/j.conbuildmat.2021.123917.

[40] R. Liang, Y. Huang, and Z. Xu, "Experimental and Analytical Investigation of Bond Behavior of Deformed Steel Bar and Ultra-High Performance Concrete," *Buildings*, vol. 12, no. 4, Apr. 2022, Art. no. 460, https://doi.org/10.3390/buildings12040460.

[41] M. H. Harajli, M. Hout, and W. Jalkh, "Local Bond Stress-Slip Behavior of Reinforcing Bars Embedded in Plain and Fiber Concrete," *ACI Materials Journal*, vol. 92, no. 4, pp. 343–354, Jul. 1995, https://doi.org/ 10.14359/999.

[42] T. Sripan *et al.*, "Assessment of bonding strength of steel bar in recycled aggregate concrete containing ground palm oil fuel ash," *Innovative Infrastructure Solutions*, vol. 9, no. 3, Feb. 2024, Art. no. 59, https://doi.org/10.1007/s41062-023-01360-x.

[43] A. Qasem, Y. S. Sallam, H. Hossam Eldien, and B. H. Ahangarn, "Bond-slip behavior between ultra-high-performance concrete and carbon fiber reinforced polymer bars using a pull-out test and numerical modelling," *Construction and Building Materials*, vol. 260, Nov. 2020, Art. no. 119857, https://doi.org/10.1016/j.conbuildmat.2020.119857.

[44] A. Al-Hamrani and W. Alnahhal, "Bond durability of sand coated and ribbed basalt FRP bars embedded in high-strength concrete," *Construction and Building Materials*, vol. 406, Nov. 2023, Art. no. 133385, https://doi.org/10.1016/j.conbuildmat.2023.133385.

[45] A. Abushanab and W. Alnahhal, "Bond strength of corroded reinforced recycled aggregate concrete with treated wastewater and fly ash," *Journal of Building Engineering*, vol. 79, 2023, Art. no. 107778, https://doi.org/10.1016/j.jobe.2023.107778.